Development of a Fitting Model Suitable for the Isothermal Titration Calorimetric Curve of DNA with Cationic Ligands

Wankee Kim,[†] Yuichi Yamasaki,*[,†] and Kazunori Kataoka*[,†,‡]

Department of Materials Science and Engineering, School of Engineering, The University of Tokyo, 7-3-1 Hongo, Bunkyo-ku, Tokyo 113-8656, Japan, and Center for Disease Biology and Integrative Medicine, Graduate School of Medicine, The University of Tokyo, 7-3-1 Hongo, Bunkyo-ku, Tokyo 113-0033, Japan

Received: December 28, 2005; In Final Form: April 12, 2006

A novel curve fitting model was developed for the isothermal titration calorimetry (ITC) of a cationic ligand binding to DNA. The ligand binding often generates a DNA conformational change from an elongated random coil into a compact collapsed form that is referred to as "DNA condensation". The ligand binding can be classified into two regimes having different binding constants K_i, i.e., the binding to an elongated DNA chain with a binding constant K_1 and with K_2 that occurred during the conformational transition. The two-variable curve fitting models are usually bound by a strict regulation on the difference in the values of the binding constants $K_1 > K_2$. For the DNA condensation, however, the relationships for K_1 and K_2 are still unclear. The novel curve fitting model developed in this study takes into account this uncertainty on the relationship of the binding constants and is highly flexible for the two-variable binding constant system.

Introduction

Isothermal titration calorimetry (ITC) is a useful method to explore the interaction between DNA and cationic ligands.[1−10] By adding a solution of cationic ligands to a DNA solution, the ITC instrument measures the heat accompanied by the binding reaction. The thermodynamic parameters such as changes in enthalpy, entropy, and free energy can be obtained by fitting the ITC curve to an adequate curve fitting model. Nevertheless, general curve fitting models are useful only for simple binding systems, and they may not be applied to particular cases such as DNA condensation.

In general, there are three kinds of curve fitting models, i.e., the single set of identical sites (SSIS) model, two sets of independent sites (TSIS) model, and sequential binding sites (SBS) model.[11,12] The SSIS model satisfies many ligand binding systems when all the binding sites on the substance are identical. The following parameters, stoichiometry N, binding constant K, and change in enthalpy ΔH can be obtained using this fitting model. The TSIS model, which is useful when substances have two kinds of binding sites, enables us to calculate both sets of parameters N_1, K_1, ΔH_1 and N_2, K_2, ΔH_2 for the first and second ligand bindings. While the TSIS model seems to be well adapted to various cases, it should not be applied to the particular system where K_1 is smaller than K_2, because this model is constructed assuming that K_1 is larger than K_2. The SBS model is appropriate for the system, such as the binding of multiple ligands to transition metal ions, for example, the binding of four Br^- ions to Cd^{2+} leading to $CdBr_4^{2-}$. For this case, the number of sequential sites should be integral. The absence of a parameter equivalent to N indicates that the curve fitting is carried out by changing only two parameters, K and H, on each site.

Concerning the binding of cationic ligands to DNA, a conformational change in the DNA chain may affect their binding behavior. The DNA chain collapses after some fraction of negative charges on the phosphate backbone is neutralized by cationic ligands, which is referred to as DNA condensation. The binding process of cationic ligands to DNA can be classified into two parts, a simple binding without a DNA conformational transition and another binding event that followed during the conformational transition. The binding constant for the former is K_1 and that for the latter is K_2. During the beginning of ligand binding, the former binding process proceeds where the DNA chains retain their conformation. Consequently, the latter binding occurs after the former was completed, resulting from the DNA conformational transition.

This scheme is consistent with the prediction of the counterion condensation (CC) theory developed by Oosawa and Manning and with the experimental results obtained from electrophoresis.[13] The CC theory indicates the presence of critical residual charges on elongated DNA chains that results from the former ligand binding. While the degree of charge neutralization depends on the ligand concentration, the critical value of charge neutralization is determined by their valence. For example, the values of DNA in the presence of monovalent, divalent, and trivalent cations are 0.76, 0.88, and 0.92, respectively.[14] Bloomfield concluded that the DNA chains retain their conformation until the degree of charge neutralization is increased to 0.90, indicating that cationic ligands with their valence equal to or grater than 3 possesses the potential to generate DNA condensation. On the contrary, it was clarified that almost all of the negative charges are neutralized in the collapsed state.[15] These experimental results suggest that the DNA conformation and its residual charges correlate with each other, and that the binding manner of the cationic ligands is also affected by DNA conformation. Therefore, the binding classification described above is appropriate for the ligand binding to DNA phosphates.

* To whom correspondence should be addressed: Kazunori Kataoka, tel +81-3-5841-7138, fax +81-3-5841-7139, e-mail kataoka@bmw.t.u-tokyo.ac.jp; Yuichi Yamasaki, tel +81-3-5841-7145, fax +81-3-5841-7139, e-mail yamasaki@bmw.t.u-tokyo.ac.jp.

† Department of Materials Science and Engineering, School of Engineering, The University of Tokyo.

‡ Center for Disease Biology and Integrative Medicine, Graduate School of Medicine, The University of Tokyo.

10.1021/jp057554e CCC: $33.50
Published on Web 05/17/2006

To obtain thermodynamic parameters from the ITC measurements, the suitable fitting model should be carefully chosen by considering the relationship of the magnitude of the binding constants. For the DNA condensation, however, this relationship has so far been unknown. Recently, Teif and Lando theoretically pointed out that the DNA conformational change to the collapsed state takes place when $K_2 > K_1$.[16] Actually, Mel'nikov et al. reported the cooperative binding observed in the transition region of the DNA condensation induced by a cationic surfactant.[17] Thus, we developed a novel fitting model suitable for this situation $K_2 > K_1$ to analyze the binding isotherm obtained from the DNA condensation. In this paper, the binding isotherms obtained from the DNA condensation induced by a low molecular weight condensing reagent, cobalt hexamine ($Co(NH_3)_6^{3+}$), and by a polymeric cation poly(ethylene glycol)−poly(L-lysine) block copolymer (PEG−PLL), are demonstrated as typical examples. The former is treated as a standard chemical of a DNA condensation investigation[18] and the latter as a promising polycation as a gene carrier.[19] A comparison of both binding isotherms and the validity of the novel fitting model will be discussed in detail.

Experimental Section

Materials. The plasmid pGL3 DNA (5256 base pairs) was purchased from Promega (Madison, WI). The plasmid DNA (pDNA) was amplified in competent DH5α *Escherichia coli* and purified using the Qiafilter giga kit (QIAGEN, Germany). A stock solution of pDNA was prepared by dissolving purified pDNA in Millipore grade water containing 10 mM NaCl without any buffer solution. The DNA concentration was determined by the absorption at 260 nm. The PEG−PLL block copolymer with the average PEG molecular weight of 12 000 and the average degree of lysine polymerization of 109 was used in this study. The PEG−PLL block copolymer was prepared as already prescribed.[20] Let us now briefly explain the synthesis. PEG−PLL was synthesized using α-methoxy-ω-amino-PEG to initiate polymerization of the *N*-carboxy anhydride of the *Z*-protected lysine. The length of the lysine segment was regulated by the ratio of the monomer to PEG initiator. The deprotection of lysine was carried out under acidic conditions. ^{1}H NMR and size exclusion chromatography were employed for characterization of this block copolymer. The degree of polymerization is deduced by the ratio of the methylene proton of PEG to that on the lysine residue. Cobalt(III) hexamine trichloride was obtained from Wako Pure Chemicals (Osaka, Japan) and used as received.

Isothermal Titration Calorimetry. Isothermal titration calorimetry (ITC) was performed using a Microcal VP-ITC calorimeter (Northampton, MA) with the normal cell (1.4643 mL) at 30 °C. Two milliliters of pDNA solution (0.3 mM in phosphate) was poured inside the cell after three rinses with 10 mM NaCl solution. The condensing agents were titrated into the pDNA solutions using an injection syringe. The concentrations of cobalt hexamine and PEG−PLL were chosen to be 1.2 and 3 mM (in lysine unit), respectively. Each titration consisted of a preliminary 1-μL injection followed by 29 subsequent 10-μL injections at 3-min intervals. Control experiments were carried out for both ligands to determine the heats of ligand dilution, because the dilution effect should be subtracted to obtain the heat of binding. Prior to the ligand binding experiments, the calorimeter was verified by carrying out the Tris base protonation reaction with hydrochloric acid ($\Delta H = -13.58$ kcal/mol).

Analysis of ITC Curve. The analysis of the obtained ITC curves was performed using origin software with version 5.0 attached to the instrument. First, the integrated ITC curves were obtained from the raw data of the power change at each injection, using the add-on module for the purpose in the software, and then the fittings of those data to the fitting function developed here were performed to obtain the thermodynamic parameters, using a fitting tool prepared in the software, which was based on the Levenberg−Marquardt nonlinear fitting algorithm.

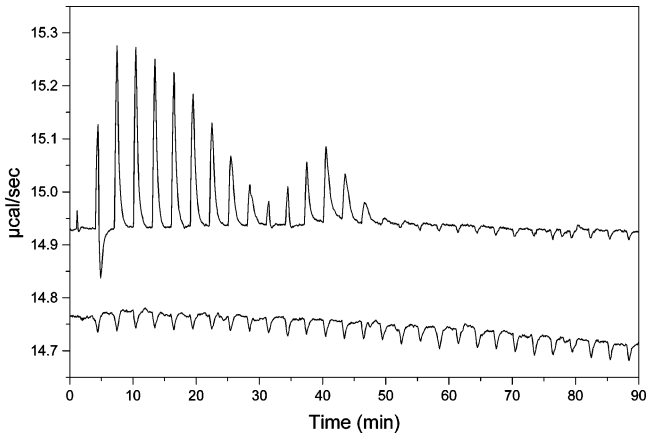

Figure 1. Raw data of ITC measurement for cobalt hexamine binding to plasmid pGL3 DNA in 10 mM NaCl aqueous solution. The upper curve shows the heats resulting from the titration of cobalt hexamine to pDNA solution. The lower curve was obtained by the titration without pDNA, indicating the heats generated by the dilution of the ligand solution. To obtain the ITC binding curves, the lower one should be subtracted from the upper one.

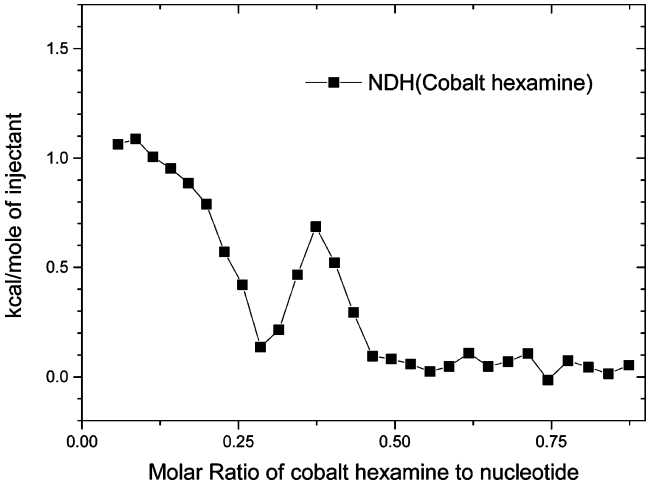

Figure 2. Integrated ITC curve of cobalt hexamine binding to plasmid pGL3 DNA in 10 mM NaCl aqueous solution. This ITC binding curve was calculated from both curves in Figure 1. Endothermic two-stage binding was observed during this ligand binding.

Results

Typical nonintegrated titration curves are shown in Figure 1. The upper curve was obtained by titrating pDNA with cobalt hexamine, and the lower curve was obtained without pDNA indicating the heat of the dilution of cobalt hexamine solution. The upper curve includes the heats resulting from both the dilution effect and the binding reaction. To obtain integrated binding curves as shown in Figure 2, the peaks of both curves were integrated and the latter was subtracted from the former. Figure 2 indicates that the binding of cobalt hexamine onto pDNA can be classified into two stages. Endothermic events were observed during both stages, suggesting that this binding

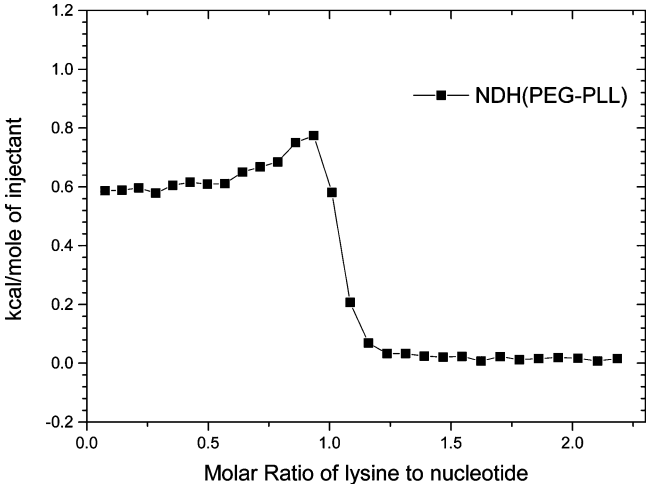

Figure 3. Integrated ITC curve of PEG−PLL binding to plasmid pGL3 DNA in water with 10 mM NaCl. The endothermic binding was completed by the charge ratio of 1.2.

was entropically driven. This result is in good agreement with those reported by other researchers.[2,4]

In this system, the initial binding stage was completed with the charge ratio of 0.9. The second stage was observed when a further addition of cobalt hexamine occurred. No heat was generated at the region in the charge ratio range higher than 1.5. From the results of turbidity measurement, a significant decrease in the transmittance resulting from the formation of aggregates was observed immediately following the second binding stage (data not shown). After the titration measurement, precipitates were visually observed in the sample solution.

The integrated ITC curve of the PEG−PLL binding to pDNA is shown in Figure 3, indicating an endothermic ligand binding the same as that observed in the $Co(NH_3)_6^{3+}$/pDNA system. Although the two-stage binding observed in the ITC curve of the cobalt hexamine titration is well separated, no segregation was observed in the ITC profile for the PEG−PLL/pDNA system. The PEG−PLL binding was completed with the charge ratio of 1.2.

Development of the Novel Fitting Model

A novel fitting model is based on the combination of the single set of identical sites (SSIS) model. Let us introduce the SSIS model as follows.[11,12] Generally, the binding constant K and the relationship of the total and free ligand concentrations (X_t and $[X]$) are represented by eqs 1 and 2, respectively

$$K = \frac{\Theta}{(1-\Theta)[X]} \tag{1}$$

$$X_t = [X] + N\Theta M_t \tag{2}$$

where N is the number of binding sites, M_t is the total concentration of macromolecule, and Θ is the fractional sites occupied by ligand. Combining eqs 1 and 2 gives eq 3

$$\Theta^2 - \Theta\left[1 + \frac{X_t}{NM_t} + \frac{1}{NKM_t}\right] + \frac{X_t}{NM_t} = 0 \tag{3}$$

The total heat content Q of the solution contained in the sample cell at fractional saturation Θ is

$$Q = N\Theta M_t \Delta H V_o \tag{4}$$

where ΔH is the molar heat of ligand binding and V_o is the cell

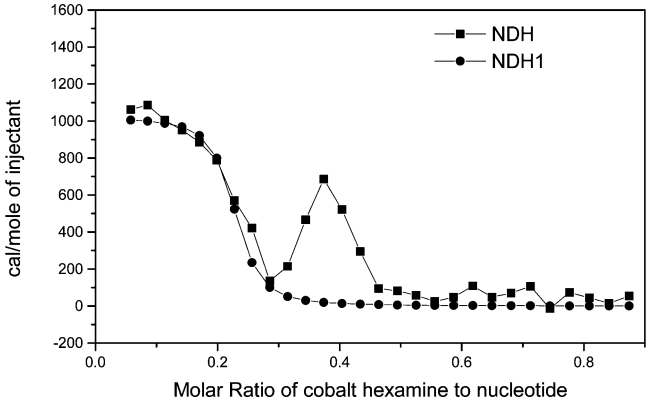

Figure 4. Integrated ITC curve of cobalt hexamine binding to plasmid pGL3 DNA (■) and representative ITC curve NDH1 generated from the SSIS model with the following fitting parameter (●). $N_1 = 0.216 \pm 0.004$, $K_1 = (17.79 \pm 4.99) \times 10^5\ M^{-1}$, $\Delta H_1 = 1019 \pm 30$ cal/mol.

volume. Solving the quadratic eq 3 for Θ and then substituting this into eq 4 gives eq 5

$$Q = \frac{NM_t\Delta HV_o}{2}[1 + (X_t/NM_t) + (1/NKM_t) - \sqrt{(1 + (X_t/NM_t) + (1/NKM_t))^2 - (4X_t/NM_t)}] \tag{5}$$

The value of Q can be calculated for any designated values of N, K, and ΔH at the end of the ith injection and designated $Q(i)$. The parameter of interest for comparison with the experiment, however, is the change in heat content from the completion of the $(i-1)$th injection to completion of the i-th injection. The expression for Q in eq 5 only applies to the liquid contained in volume V_o. Therefore, after an injection is completed, it is obvious that a correction must be made for the displaced volume (i.e., ΔV_i = injection volume) since some of the liquid in V_o after the $(i-1)$th injection will no longer be in V_o after the ith injection, even though it will contribute to the heat effect (assuming that the kinetics of the reaction and mixing are fast) before it passes out of the working volume V_o. The liquid in the displaced volume contributes about 50% as much heat effect as an equivalent volume remaining in V_o. The correct expression for the heat released $\Delta Q(i)$ from the ith injection is

$$\Delta Q(i) = Q(i) + \frac{dV_i}{V_o}\left[\frac{Q(i) + Q(i-1)}{2}\right] - Q(i-1) \tag{6}$$

By dividing $\Delta Q(i)$ with moles in the ith injected volume, the normalized heat, NDH(i), is obtained. Hereafter, NDH(i) is described by NDH(N, ΔH, K) because NDH(i) is dependent on the three parameters, N, ΔH and K.

A set of fitting parameters, N_1, K_1, and ΔH_1, is assigned to the initial binding stage of cationic ligands to the elongated pDNA, and another set, N_2, K_2, and ΔH_2, is assigned to the second binding stage during the pDNA conformational transition. On the basis of the SSIS model, the optimum fitting parameters for the initial stage provide the most suitable ITC curve as shown in Figure 4.

On comparison of the ITC curves for the PEG−PLL/pDNA system with that for $Co(NH_3)_6^{3+}$/pDNA, the molar ratios where the second binding stage appeared disagree. It is assumed that the second binding stage in the PEG−PLL system is immediately generated after the initial binding stage. In the system of cobalt hexamine, however, the generation of the second stage requires an excess amount of ligand in the bulk solution, corresponding to the delay of the second stage in Figure 2. As

shown in Figure 3, the second stage in the PEG−PLL system was almost finished around the charge equivalent condition. Therefore, both the initial and second binding stages in the PEG−PLL system coexist in a certain region where the molar ratio is greater than 0.5. This binding feature agrees with the results obtained from the direct observation of the DNA condensation using fluorescence microscopy.[21]

On the contrary, the two binding stages were well separated in the system of cobalt hexamine. In this system, the second binding stage during the DNA conformational change occurs after the initial stage where the fraction of the bound ligand reaches the critical one and all of the injected cationic ligands are consumed in the initial binding stage. As the injections of the cationic ligands are repeated, the amount of bound ligands gradually increases and reaches a maximum value at the molar ratio of 0.3, corresponding to the critical residual charges of the elongated DNA double helices, i.e., the end point of the initial binding stage. Under this condition, the added ligands do not tend to bind the elongated DNA, then the heat generated by the binding gradually decreases. The further addition of cationic ligands induces the DNA conformational change or "DNA condensation". During this transition, the second binding stage of the cationic ligands is promoted. The presence or absence of the delay between the two binding stages seems to be a significant phenomenological difference. Therefore, the effect of this delay is taken into consideration in the novel fitting model developed in this study.

Prior to describing the delay of the second binding stage observed in the $Co(NH_3)_6^{3+}$/pDNA system, the curve fitting for the second binding stage should be discussed here. On the basis of the SSIS model, a general ITC curve should be produced as a decreased sigmoidal curve as shown in Figure 4 (NDH1). According to the results of the DNA conformational analysis under fluorescence microscopy, both the elongated and collapsed DNA chains coexist during the transition region of the DNA condensation.[22] Thus, the population of collapsed DNAs should gradually increase with an increase in the molar ratio. This leads to the decrease in the fraction of ligands bound to the elongated DNA and the increase in that of the collapsed one. If the delay in the second binding stage was missing, the residual ligands not involved in the initial binding stage ideally contribute to the second binding stage. The amount of this residual ligand is represented by differences between the maximum and each fraction of the binding ligand, which can be expressed by an increased sigmoidal curve. Because the sigmoidal NDH having N, K, ΔH as a variable is linearly dependent on the fraction of ligands (Θ), Θ can be described as the absolute value of NDH divided by ΔH, ABS(NDH/ΔH).

To describe the fraction of the occupied site on DNA during the second binding stage, an NDH3 sigmoidal curve was employed. The definition of parameters for NDH3 is basically the same as those for the NDH1, but only N_3 is variable when considering the delay of the second binding stage. When N_3 is equal to N_1, the initial binding stage is immediately followed by the second binding stage during the DNA condensation. On the contrary, as N_3 becomes larger than N_1, the second binding stage is separated from the initial binding stage, indicating that the delay in the second stage is significant in the ITC curve. Thus, the fraction of the occupied site on DNA during the second stage is represented by ABS((ΔH_1 − NDH3)/ΔH_1) in Figure 5, which is derived from 1 − ABS(NDH3/ΔH_1). We intend to generate for the second binding stage the NDH2 curve which is a function of N_2, K_2, and ΔH_2. The second binding stage of the ITC curve was fitted by the product of the

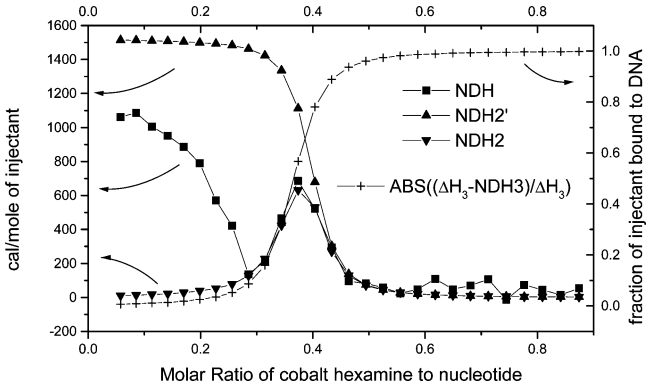

Figure 5. Representative curve for the second binding stage during pDNA condensation (NDH2; ▼).

hypothetical ITC curve NDH2′ and the increased sigmoidal curve ABS((ΔH_1 − NDH3)/ΔH_1). The ITC curve NDH2′ that corresponds to a standard ITC curve with the absence of the initial binding stage is generated by the SSIS model, indicating that the NDH2′ curve is defined by N_2', K_2', and $\Delta H_2'$. The product was defined as NDH2 where N_2' − N_3 (the difference of N_2' and N_3), K_2', and $\Delta H_2'$ are selected for N_2, K_2, and ΔH_2, respectively.

Application of New Model

The optimum fittings for the experimental ITC curves of both $Co(NH_3)_6^{3+}$/pDNA and PEG−PLL/pDNA are shown in Figures 6 and 7, respectively. The ITC curves were fitted by the sum of NDH1 and NDH2, corresponding to the initial and second binding stages, respectively. The sum of these two curves represents the relation of the total heats accompanied by ligand binding on DNA to the mixing ratio. Although the curve NDH1 is defined by the set of three parameters, N_1, K_1, and ΔH_1, another curve, NDH2, was defined by the set of six parameters, N_3, K_1, ΔH_1, N_2', K_2', and $\Delta H_2'$. In this method, both curves, NDH1 and NDH2, were simultaneously fitted. The difference in N_2' and N_3, which is described by N_2, means the binding stoichiometry for the second binding stage in the novel fitting model, and the difference in N_1 and N_3 reflects the delay of the second binding stage. The important thermodynamic parameters are listed in Tables 1 and 2. For both the simplified notation and comparison with the reported data, the binding stoichiometry for the second binding stage is represented by the parameter N_2 in the tables.

Discussion

The cooperative binding of polycations to DNA chains has been discussed as a typical binding feature of polyelectrolytes. Similar binding processes have already been independently considered by McGhee and von Hippel[23] and by Schwarz.[24] MaGhee and von Hippel suggested the concept of cooperativity of protein binding to DNA using the following three binding modes: (1) the binding to the isolated site with an intrinsic binding constant K, (2) a singly contiguous site to which a linear polymer binds with binding constant $K\omega$, and (3) a doubly contiguous site to which a linear polymer binds with binding constant $K\omega^2$, where ω is the cooperativity constant. When $\omega > 1$, the cationic ligands attract each other and the binding is positively cooperative; when $\omega < 1$, the cationic ligands repel each other and the binding is anti or negatively cooperative; when $\omega = 1$, neither cooperativity is observed during the binding.

Schwarz's theory also implies two types of intrinsic binding processes: (1) the binding of isolated ligands with binding

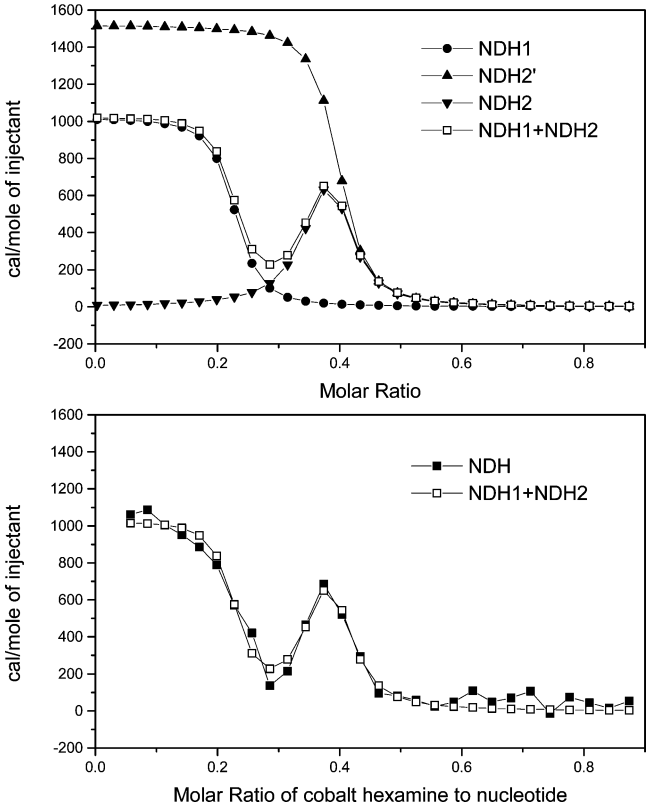

Figure 6. Optimum fitting for the experimental ITC curve (■) of $Co(NH_3)_6^{3+}$/pDNA, NDH1 + NDH2 (□). NDH1 (●) represents the initial binding stage corresponding to that in Figure 4. NDH2′ (▲) and NDH2 (▼) are the same as those in Figure 5. NDH1 + NDH2 is used for the fitting of the experimental ITC curve; $N_1 = 0.216 \pm 0.004$, $K_1 = (17.79 \pm 4.99) \times 10^5\ M^{-1}$, $\Delta H_1 = 1019 \pm 30$ cal/mol, $N_2' = 0.385 \pm 0.012$, $N_3 = 0.354$, $N_2 = N_2' - N_3 = 0.031 \pm 0.012$, $K_2 = K_2' = (27.82 \pm 12.61) \times 10^5\ M^{-1}$, $\Delta H_2 = \Delta H_2' = 1520 \pm 301$ cal/mol.

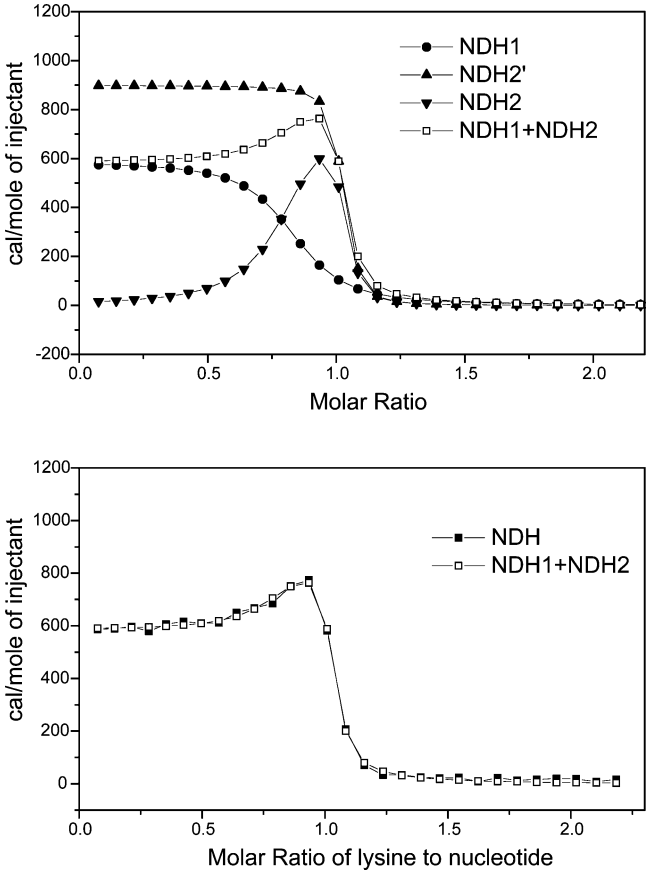

Figure 7. Optimum fitting for the experimental ITC curve (■) of PEG−PLL/pDNA, NDH1 + NDH2 (□). NDH1 (●) represents the initial binding stage corresponding to those of the PEG−PLL/pDNA system shown in Figures 5 and 6. NDH2′ (▲) and NDH2 (▼) correspond to those in Figure 6. NDH1 + NDH2 is used for the fitting of the experimental ITC curve: $N_3 = N_1 = 0.810 \pm 0.026$, $K_1 = (2.66 \pm 0.62) \times 10^5\ M^{-1}$, $\Delta H_1 = 585 \pm 5$ cal/mol, $N_2' = 0.994 \pm 0.005$, $N_2 = N_2' - N_3 = 0.184 \pm 0.031$, $K_2 = K_2' = (51.07 \pm 13.98) \times 10^5\ M^{-1}$, $\Delta H_2 = \Delta H_2' = 899 \pm 37$ cal/mol.

constant K (nucleation), and (2) the binding of ligands to the nearest-neighbor binding site (aggregation) with binding constant Kq, where q is the cooperativity parameter. In both models, the binding process with the binding constant $K\omega$ or Kq is generated by the initial ligand binding with binding constant K, which is the matter of our concern. Let us assume that K_2 was equal to $K\omega$ or Kq. For the cobalt hexamine binding to DNA, ω or q is estimated to be 1.56, which is obtained by K_2/K_1 using the parameters shown in Table 1. For the PEG−PLL binding to DNA, ω or q is estimated to be 19.20 using the parameters shown in Table 2. In both cases, it is obvious that the binding constant K_2 seems to be significantly enhanced and the estimation for the cobalt hexamine binding is inconsistent with the reported data.[2] Although the above classification was suggested to explain the cooperative binding of the cationic ligands, it is not clear in this study whether such kinds of cooperativities induced by the ligand−ligand interactions exist in the binding of the cobalt hexamine or PEG−PLL to pDNA.

In this study, it was assumed that the positive cooperative binding of the cobalt hexamine or PEG−PLL to DNA is attributed to the conformational change in DNA rather than the interaction between the same chemicals. The DNA conformational change produces the environmental modulation around the DNA vicinity, and this may affect the binding features of the cationic ligands. Hud et al. suggested that the effect of the DNA segment fluctuation induces the enhanced binding of cationic ligands to a loop formed by two sequence-separated sections in close contact.[25] The cationic ligands bind to this contact and stabilize the loop. Successive ligands bind both the loop and extended DNA to induce the collapsed form. Therefore, the binding constants K_1 and K_2 are treated as individual variables in this study.

To develop a flexible fitting method, different types of ligands, a low-molecular weight metal complex cobalt hexamine and block copolymer PEG−PLL, were employed in this study. Cobalt hexamine is a widely used chemical as a standard reagent of DNA condensation. On the contrary, PEG−PLL is a relatively recently developed reagent as a gene carrier.[19] As exemplified by the presence or absence of the delay in the appearance of the second binding stage in Figures 2 and 3, the condensation mechanism seems to be slightly different from each other despite the same driving force, the electrostatic interaction. It was reported that this difference becomes enhanced in the dilute DNA solution experiments and the latter more effectively induces the DNA condensation.[21]

Under such situations, the charge equivalent mixing ratio between PEG−PLL and DNA is enough to induce the DNA condensation, while an excess amount of cobalt hexamine, at least several times that of the phosphate residue, should be required. A similar trend was observed in the ITC curves obtained in this study. The charge ratio at the end point of the PEG−PLL titration was 1.2, while that of cobalt hexamine was slightly higher than this value. This difference was mainly caused by their chemical structures. In this study, a simple comparison of the thermodynamic parameters N_1 and K_1 in the

TABLE 1: Parameters Obtained by Various Fitting Methods

	N_1	$K_1/10^5$ (M^{-1})	ΔH_1 (cal/mol)	N_2	$K_2/10^5$ (M^{-1})	ΔH_2 (cal/mol)
this work[a]	0.216 ± 0.004	17.79 ± 4.99	1019 ± 30	0.031 ± 0.012	27.82 ± 12.61	1520 ± 301
ref 2[b]	0.217 ± 0.012	2.30 ± 0.80	1240 ± 100	0.059 ± 0.012	6.00 ± 1.60	820 ± 90
origin[c]	0.218 ± 0.010	74.02 ± 142.4	1086 ± 68	not converged		

[a] This work: developed by this work. [b] ref 2: reported in reference 2. [c] Origin: by applying the two sets of independent sites (TSIS) model to each binding process divided from the experimental ITC curve shown in Figure 2, which is the same method as that used in the ref 2. $N_2' = 0.385 \pm 0.012$, $N_3 = 0.354$, $N_2 (= N_2' - N_3) = 0.031 \pm 0.012$, $K_2 = K_2'$, $\Delta H_2 = \Delta H_2'$.

TABLE 2: Parameters Obtained by Various Fitting Methods

	N_1	$K_1/10^5$ (M^{-1})	ΔH_1 (cal/mol)	N_2	$K_2/10^5$ (M^{-1})	ΔH_2 (cal/mol)
this work[a]	0.810 ± 0.026	2.66 ± 0.62	585 ± 5	0.184 ± 0.031	51.07 ± 13.98	899 ± 37
origin[b]	0.781 ± 0.032	139.10 ± 44.19	584 ± 9	0.222 ± 0.034	7.2 ± 2.23	973 ± 77

[a] This work: developed by this work. [b] Origin: by applying TSIS model to the ITC curve shown in Figure 3. $N_3 = N_1$, $N_2' = 0.994 \pm 0.005$, $N_2 (= N_2' - N_3) = 0.184 \pm 0.031$, $K_2 = K_2'$, $\Delta H_2 = \Delta H_2'$.

cobalt hexamine system with those of PEG−PLL makes no realistic sense, because the former was analyzed in a molar unit and the latter was summarized in a charge unit. On comparison of N_1 with the consideration of the valency, however, it is obvious that PEG−PLL more effectively binds (see Tables 1 and 2).

In the novel fitting model developed in this study, the cationic ligand binding to DNA was classified into two stages, the initial and second binding stages. The former has the binding constant K_1 and the latter K_2. Regarding the magnitude relationship of the binding constants, Teif and Lando theoretically pointed out that the DNA conformational change to the collapsed state takes place when $K_2 > K_1$.[16] In the general curve fitting models for the experimental ITC curves, however, this assumption could not be taken into consideration. Although general fitting models that can treat multiple binding sites have the assumption $K_1 > K_2$, our model is not restricted by this assumption. To treat two binding stages as individual events, they were characterized in relation to the conformational change in pDNA. Thus, the former occurs when the DNA conformation retained as the elongated state and the latter is promoted during the DNA conformational change.

Generally, there is a significant difficulty in the separation of the two binding stages, when the overlap of the initial and second binding stages was observed as shown in the PEG−PLL system. Despite the absence of the saddle point in the integrated ITC curve for the PEG−PLL system, the assumption of two-stage binding is plausible, because the discrete transition between the elongated and collapsed states was essentially the same as that observed in the cobalt hexamine system.[21] Table 1 shows a comparison of the thermodynamic parameters determined in this study with those by other methods reported in ref 2 and obtained by the manufacturer recommended method that is based on the two sets of independent sites (TSIS) model. Although the second set of parameters did not converge using the TSIS model, no significant difference was observed in both values of N_1 and N_2. As mentioned in the Introduction, the TSIS model should not be applied to the particular system where K_1 is smaller than K_2, because this model is constructed assuming that K_1 is greater than K_2. This is the reason the second set of parameters was not determined by the TSIS model.

Matulis et al. also employed the TSIS model, but they completely divided the integrated ITC curve by the saddle point. In their method, two parts of the ITC curve were separately fitted.[2] Therefore, the magnitude relationship of K_1 and K_2 would not be discussed under their framework. On the contrary, both parts were simultaneously fitted in this study. In addition, when their method was applied to the PEG−PLL system, the curve fitting was done under the restricted assumption $K_1 > K_2$. However, our method is not restricted by this assumption. Among these three methods, thus, an appropriate method suitable for the discussion on the magnitude relationship of K_1 and K_2 is considered to be limited to the novel method developed in this study.

The charge ratio of the cationic ligands to DNA is expressed by the total stoichiometry, the sum of N_1 and N_2. On the basis of the consideration of the valence of cobalt hexamine, the charge ratio is estimated to be 0.72 in this study, suggesting that the residual ligands do not directly contribute to the DNA condensation (see Table 1). This trend is consistent with another report.[2] It is still controversial that the results of the ITC experiments disagree with the theoretical prediction of the two-variable counterion condensation theory.[14] As for the PEG−PLL system, the charge ratio was determined to be 0.99, indicating that almost all of the negative charge of the DNA phosphate is neutralized by the ligand binding (see Table 2). The result of the charge equivalent complexation agrees with those obtained from the single molecule observation under fluorescence microscopy.[20] This difference in the binding stoichiometry between cobalt hexamine and PEG−PLL reflects the strength of the electrostatic interaction between the cationic ligands and DNA phosphates.

Conclusion

The novel fitting method based on the SSIS model for the experimental ITC curve was developed and applied to the cationic ligands binding to DNA, cobalt hexamine, and PEG−PLL systems in this study. It is demonstrated that this curve fitting method can be applicable for both systems. As for the cobalt hexamine system, the thermodynamic parameters obtained by the novel fitting method have a similar trend with those reported by other researchers. It was suggested that this method is applicable for the PEG−PLL system, in which the separation of the two binding events is not enough for the appearance of the experimental ITC curve. Although other fitting methods are applicable under the restricted assumption $K_1 > K_2$, our method, unrestricted by this assumption, is widely applicable for both cases, $K_1 > K_2$ and $K_2 > K_1$.

Acknowledgment. We thank Mr. S. Fukushima of Nippon Kayaku Co., Ltd., Japan, for the kind donation of the PEG−PLL block copolymer. This work was partially supported by a grant-in-aid for scientific research from the Ministry of Education, Culture, Sports, Science, and Technology of Japan (MEXT), the Core Research Program for Evolutional Science and Technology (CREST) from the Japan Science and Technol-

ogy Agency (JST), and 21st century COE program "Human-Friendly Materials based on Chemistry" from MEXT.

References and Notes

(1) Spink, C. H.; Chaires, J. B. *J. Am. Chem. Soc.* **1997**, *119*, 10920−10928.
(2) Matulis, D.; Rouzina, I.; Bloomfield, V. A. *J. Mol. Biol.* **2000**, *296*, 1053−1063.
(3) Bronich, T.; Kabanov, A. V.; Marky, L. A. *J. Phys. Chem. B* **2001**, *105*, 6042−6050.
(4) Matulis, D.; Rouzina, I.; Bloomfield, V. A. *J. Am. Chem. Soc.* **2002**, *124*, 7331−7342.
(5) Pozharski, E.; MacDonald, R. C. *Biophys. J.* **2002**, *83*, 556−565.
(6) Keller, M.; Tagawa, T.; Preuss, M.; Miller, A. D. *Biochemistry* **2002**, *41*, 652−659.
(7) Keller M.; Jorgensen, M. R.; Perouzel, E.; Miller, A. D. *Biochemistry* **2003**, *42*, 6067−6077.
(8) Ehtezazi, T.; Rungsardthong, U.; Stolnik, S. *Langmuir* **2003**, *19*, 9387−9394.
(9) Rungsardthong, U.; Ehtezazi, T.; Bailey, L.; Armes, S. P.; Garnett, M. C.; Stolnik, S. *Biomacromolecules* **2003**, *4*, 683−690.
(10) Nisha, C. K.; Manorama, S. V. *Langmuir* **2004**, *20*, 2386-2396.
(11) Freire, E.; Mayorga, O. L.; Straume, M. *Anal. Chem.* **1990**, *62*, 950A-959A.
(12) ITC Data Analysis in Origin, Ver.5.0; MicroCal, Inc.: Studio City, CA, 1998; pp 73−78.
(13) (a) Oosawa, F. *Polyelectrolytes*; Marcel Dekker: New York, 1971. (b) Manning, G. S. *Q. Rev. Biophys.* **1978**, *11*, 179−246.
(14) Wilson, R. W.; Bloomfield, V. A. *Biochemistry* **1979**, *18*, 2192−2196.
(15) Yamasaki, Y.; Teramoto, Y.; Yoshikawa, K. *Biophys. J.* **2001**, *80*, 2823−2832.
(16) Teif, V. B.; Lando, D. Y. *Mol. Biol.* **2001**, *35*, 106−107.
(17) Mel'nikov, S. M.; Sergeyev, V. G.; Yoshikawa, K. *J. Am. Chem. Soc.* **1995**, *117*, 9951−9956.
(18) Bloomfield,V. A. *Curr. Opin. Struct. Biol.* **1996**, *6*, 334−341.
(19) Katayose, S.; Kataoka, K. *Bioconjugate Chem.* **1997**, *8*, 702−707.
(20) Harada A.; Kataoka K. *Macromolecules* **1995**, *28*, 5294−5299.
(21) Yamasaki, Y.; Katayose, S.; Kataoka, K.; Yoshikawa, K. *Macromolecules* **2003**, *36*, 6276−6279.
(22) Yoshikawa, K.; Kidoaki, S.; Takahashi, M.; Vasilevskaya, V. V.; Khokhlov, A. R. *Ber. Bunsen-Ges. Phys. Chem.* **1996**, *100*, 876−880.
(23) McGhee, J. D.; von Hippel, P. H. *J. Mol. Biol.* **1974**, *86*, 469−489.
(24) Schwarz, G. *Eur. J. Biochem.* **1970**, *12*, 442−453.
(25) Hud, N. V.; Downing, K. H.; Balhorn, R. *Proc. Natl. Acad. Sci. U.S.A.* **1995**, *92*, 3581−3585.